Contains Proprietary information from SIA and Framatome

Failure Criterion Development and Parametric Finite Element Analyses to Assess Margins for the Davis-Besse RPV Head Corrosion

by

G. Wilkowski, R. Wolterman, D. Rudland, and Y.-Y. Wang
Engineering Mechanics Corporation of Columbus

April 30, 2002
to
U.S. NRC – RES

EXECUTIVE SUMMARY

This report estimates the margins that existed for the cladding in the Davis-Besse head wastage case. The margins on the calculated "failure pressure" to the operating pressure were calculated, as well as the amount of additional corrosion that had to occur for failure at the normal operating pressure.

The development of the failure criterion is first presented. The "best-estimate failure criterion" was defined as the pressure that produced the equivalent strain under biaxial loading equal to an average critical value through the thickness in the cladding. The basis of the "best-estimate failure criterion" is that the equivalent critical strain under biaxial loading corresponds to the ultimate stress in a uniaxial tension test. This resulted in the "critical equivalent strain" being 5.5 percent under biaxial loading rather than the 11.2 percent strain in the uniaxial tensile test at the start of necking. An additional consideration is needed to account for the strain gradient through the cladding thickness. When the critical strain is exceeded, then there is a redistribution of stresses that is not accounted for in the finite element analysis. To account for this lack of stress redistribution, it was assumed that failure would be reached when the average strain in the thickness exceeded the critical strain. The best-estimate "failure pressures" gave margins of 1.07 to 1.39 on the normal operating pressure. This agreed well with estimated results from the SIA analysis when the same failure criterion was used. Preliminary results from ORNL gave a higher calculated failure pressures with the same criterion, but further mesh refinement in the clad region is being pursued. The estimated additional corrosion needed to cause failure at the normal operating pressure was 0.9 to 1.8 inches more in the longest dimension when using our "best-estimate failure criterion".

The "best-estimate failure criterion" developed in this report gives calculated "failure pressures" that are about a factor of 2.2 lower than the failure criterion used in the SIA report.

These results could be affected by: (1) variable thickness (the average thickness was used in the values given above), (2) potential cladding flaws, (3) the failure strain being lower due to void growth under higher triaxial stresses causing a reduction in the ultimate strength, (4) the assumption of failure occurring when the average strain though the thickness exceeds the critical strain, (5) variability in the stress-strain curve (the curve used appeared to be an average not a minimum), and (6) a different thickness gradient along the transition from the clad region to the full head thickness than what was used.

It is recommended that the cladding to head thickness transition be documented in the metallographic work to be done once the area is cut out from the head. If a more precise assessment is desired, then the failure criterion should be explored further.

0-1

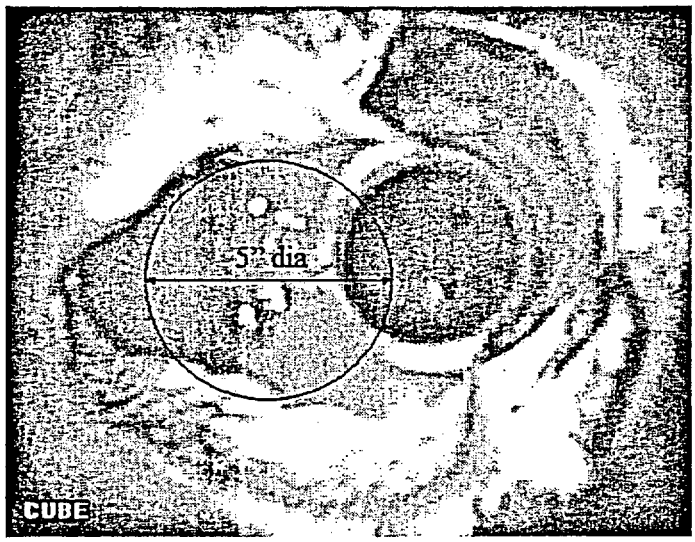

Figure 1 Photograph showing corroded area in Davis-Besse head

APPROACH

The approach undertaken in this report was to assess the cladding "failure" pressure in the corroded area using 2-dimensional finite element analysis procedures. Existing gas pipeline pipe corrosion failure models exist, but they are typically not very accurate for deep corrosion flaws.[1,2] A similar limitation exists for flaw assessment criteria in ASME Section XI, i.e., Code Case N-597. The ratio of depth of the corrosion compared to the thickness of the head was about 0.95, which is beyond the validity range of existing corrosion models.

Consequently, the approach in this effort was to conduct a number of axisymmetric finite element analyses that will allow the NRC to bound the failure pressure for the actual case. The analyses undertaken in this report involved large-deformation finite element analyses of a full reactor pressure vessel head with a single axisymmetric corrosion pit down to the cladding. The diameter of the corroded area and the thickness of the cladding were variables in these analyses.

In this case, the Davis-Besse low-alloy steel head had a thickness of 6 and 13/16 inches (including the cladding) according to FirstEnergy's submittal to NRC Bulletin 2001-01 (Docket Number 50-346). The cladding had a nominal design thickness of 3/16 inch according to the same submittal. The cladding maximum design thickness was 3/8 inch, and the design minimum thickness was 1/8 inch thick. Davis-Besse staff reported to the NRC staff that the measured cladding thickness in the corroded area had an average thickness of 0.297 inch with a minimum value of 0.24 inch.

[1] Kiefner, J. F., and Duffy, A. R., "Criteria for Determination the Strength of Corroded Areas of Gas Transmission Lines," presented at 1973 American Gas Association Transmission Conference. (Technical basis for ASME B31G.)
[2] D. Stephens and B. Leis, "Development of an Alternative Criterion for Residual Strength of Corrosion Defects in Moderate- to High-Toughness Pipe", Proceedings of 2000 International Pipeline Conference, Vol. 2, pp. 781-792, October 2000.

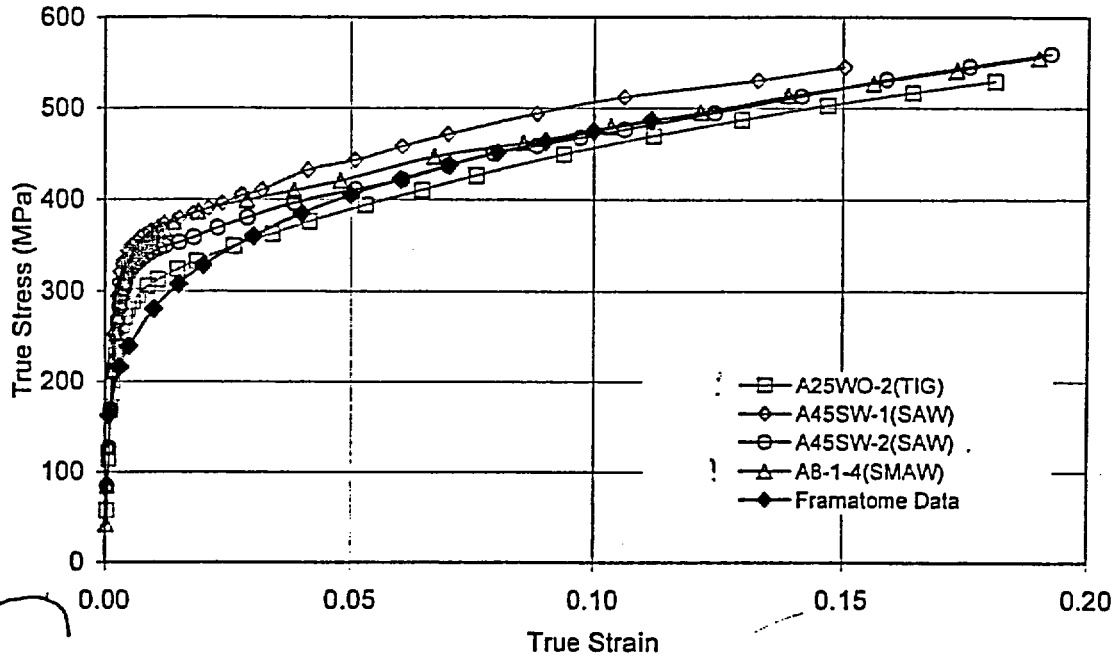

Figure 2 Comparison of TP308 weld metal uniaxial stress-strain curves (Framatome at 600F, others at 550F)

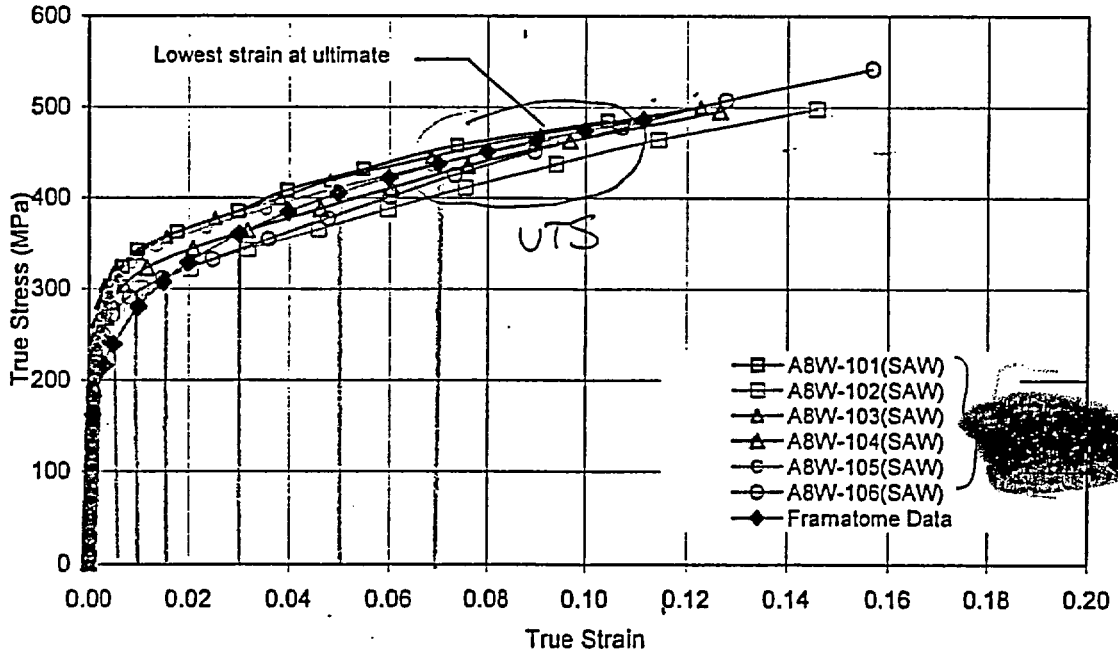

Figure 3 Comparison of TP308 weld metal uniaxial stress-strain curves (Framatome at 600F, others at 550F)

$$\sigma_1 = \sigma_x \qquad \sigma_2 = \sigma_y \qquad \sigma_3 = \sigma_z = 0 \qquad \tau_{xy} = \tau_{xz} = \tau_{yz} = 0$$

For convenience, define:

$$\sigma_2 = \lambda \sigma_1$$

The elastic strain is given by the Hooke's law for plane stress:

$$\begin{aligned} \varepsilon_{1e} &= \frac{1}{E}[\sigma_1 - \nu(\sigma_2 + \sigma_3)] = \frac{\sigma_1}{E}(1 - \nu\lambda) \\ \varepsilon_{2e} &= \frac{1}{E}[\sigma_2 - \nu(\sigma_1 + \sigma_3)] = \frac{\sigma_1}{E}(\lambda - \nu) \\ \varepsilon_{3e} &= \frac{1}{E}[\sigma_3 - \nu(\sigma_1 + \sigma_2)] = \frac{-\nu\sigma_1}{E}(1 + \lambda) \end{aligned} \tag{2}$$

Where E and ν are the elastic values of Young's modulus and Poisson's ratio, respectively.

The plastic strains are given as:

$$\begin{aligned} \varepsilon_{1p} &= \frac{1}{E_p}\left[\sigma_1 - \frac{(\sigma_2 + \sigma_3)}{2}\right] = \frac{\sigma_1}{E_p}\left(\frac{2 - \lambda}{2}\right) \\ \varepsilon_{2p} &= \frac{1}{E_p}\left[\sigma_2 - \frac{(\sigma_1 + \sigma_3)}{2}\right] = \frac{\sigma_1}{E_p}\left(\frac{2\lambda - 1}{2}\right) \\ \varepsilon_{3p} &= \frac{1}{E_p}\left[\sigma_3 - \frac{(\sigma_1 + \sigma_2)}{2}\right] = \frac{-\sigma_1}{2E_p}(1 + \lambda) \end{aligned} \tag{3}$$

Where E_p is the "plastic modulus", defined by:

$$E_p = \frac{\bar{\sigma}}{\bar{\varepsilon}_p} \tag{4}$$

$\bar{\sigma}$ = the "effective stress" (closely related to the octahedral shear stress)

$\bar{\varepsilon}_p$ = the "effective plastic strains" (closely related to the octahedral shear plastic strain)

Also, the above expression assumes that the Poisson ratio relating stress to plastic strains is 1/2, which is true for most metals.

In general:

$$\bar{\sigma} = \frac{1}{\sqrt{2}}\sqrt{(\sigma_1 - \sigma_2)^2 + (\sigma_2 - \sigma_3)^2 + (\sigma_3 - \sigma_1)^2}$$

For the particular case of plane stress ($\sigma_2 = \lambda\sigma_1, \sigma_3 = 0$):

$$\bar{\sigma} = \sigma_1\sqrt{1 - \lambda + \lambda^2} \tag{5}$$

The effective total strain is related to the effective stress and effective plastic strain according to:

If the stress state is uniaxial ($\lambda = 0$), then Eq. (8) reduces to:

$$\varepsilon_1 = \frac{\sigma_1}{E} + \left(\frac{\sigma_1}{H}\right)^{1/n}$$

$$\varepsilon_2 = \varepsilon_3 = \frac{-\nu\sigma_1}{E} - \left(\frac{1}{2}\right)\left(\frac{\sigma_1}{H}\right)^{1/n} \tag{9}$$

The equivalent strain can be calculated using the distortion energy theory definition:

$$\bar{\varepsilon} = \frac{2}{3}\sqrt{(\varepsilon_1 - \varepsilon_2)^2 + (\varepsilon_2 - \varepsilon_3)^2 + (\varepsilon_3 - \varepsilon_1)^2} \tag{10}$$

Using the above equations, the material response under uniaxial and biaxial loading can be compared. If it assumed that failure occurs at the same stress level, the decrease in failure strain due to the biaxial loading can be determined. The properties supplied by Framatome for the stainless steel TP308 weld metal are as follows:

Test temperature, F	600
0.2% yield strength, ksi	30.9
Ultimate strength, ksi	62.3
Uniform elongation	11.8%
Total elongation (not plotted)	20.6%

Using a Ramberg-Osgood curve fit the constants are as follows:

H = 115 ksi
n = 0.228

with

E = 25,570 ksi
ν = 0.295

The uniaxial stress-strain relationship is given below:

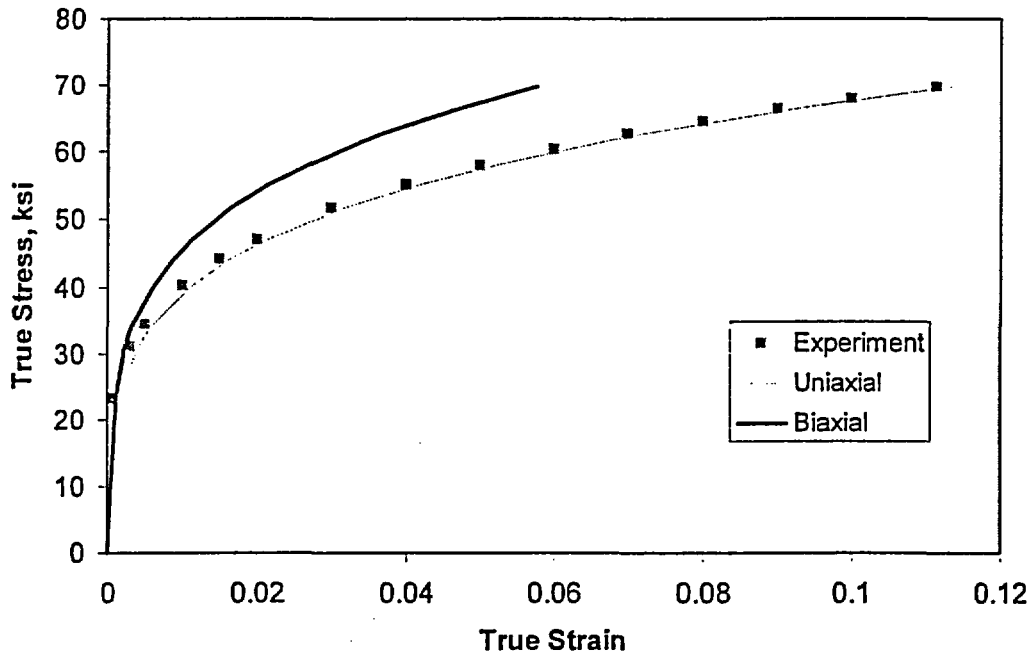

Figure 4 Comparison of uniaxial and calculated biaxial stress-strain curves for TP308 weld metal at 600F

Critical Strain Evaluation from Spherical Shell Analysis

The section describes the conditions for maximum load in uniaxial tension and conditions for maximum internal pressure for a thin-walled sphere under internal pressure, as was developed by McClintock[6]. From the maximum load conditions in this analysis, the critical strain can be determined. Since a thin-walled sphere under pressure loading is close to pure 1:1 biaxial loading, with equal stress components, this analysis provides additional support to the critical biaxial strain criterion to be used.

The conditions for maximum load in uniaxial tension is given in terms of equivalent plastic strain versus equivalent stress relation,

$$\sigma_e = \frac{d\sigma_e}{d\varepsilon_e^p} \tag{11}$$

where σ_e is the equivalent stress and ε_e^p is the equivalent plastic strain.

Assume the equivalent stress-strain relation follows the following form,

$$\sigma_e = \sigma_{e1}\left(\varepsilon_e^p\right)^n \tag{12}$$

[6] McClintock, F.A. and Argon, A.S., "Mechanical Behavior of Materials," Addison-Wesley Publishing Company, ISBN 0-201-04545-1.

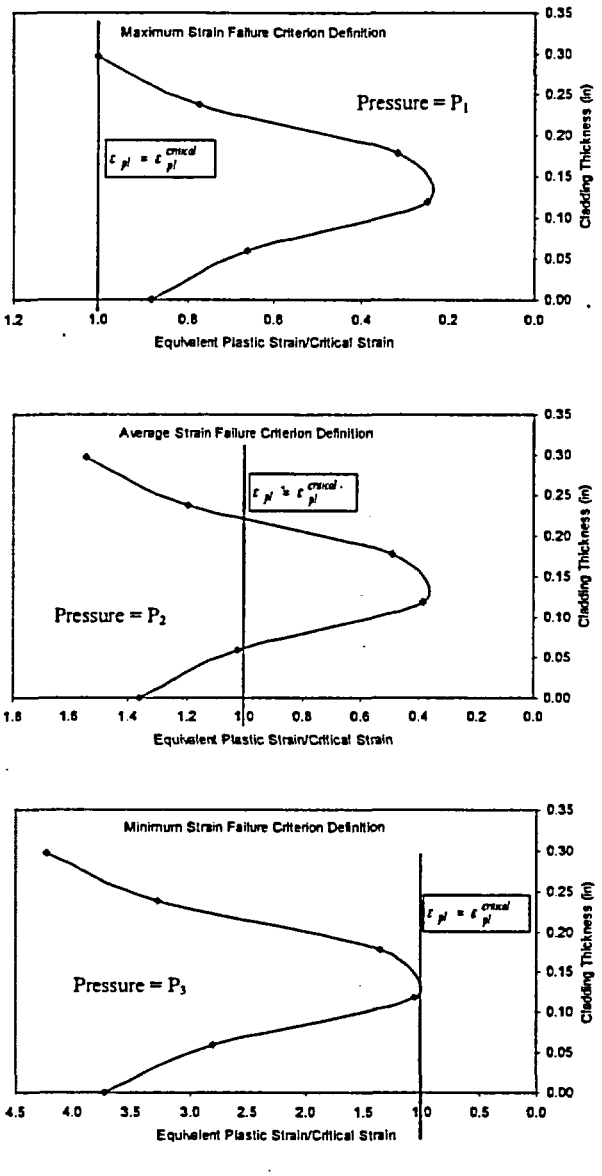

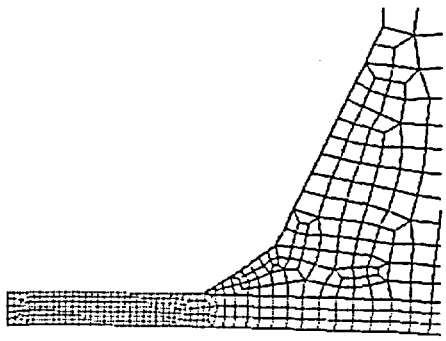

Close-up of remaining ligament of cladding showing five elements through the thickness

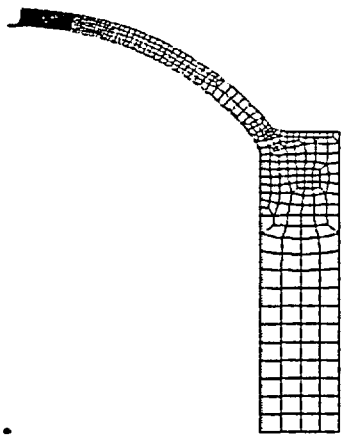

Axisymmetric finite element model showing remaining ligament at upper left corner.

Figure 5 Plots typical of the strain profile through the thickness of the cladding showing the definitions of the maximum, average, and minimum strain failure criteria based on the equivalent plastic strain through the thickness of the remaining ligament of cladding (Note: $P_1 < P_2 < P_3$)

Using the criteria of the entire ligament reaching the critical necking strain of 11.2% may over predict the failure pressure since it does not account for some of the material thinning due to void growth in the ligament and the redistribution of stresses. Using the criteria of the first point reaching the critical strain may be too conservative. The average strain through the thickness may be a reasonable "best-estimate failure criterion", but using the 11.2% strain value from the uniaxial test is too high due to the biaxial condition.

FINITE ELEMENT ANALYSIS PROCEDURES

For the Davis-Besse head analysis conducted in this report, the corrosion defect was modeled as an axisymmetric pit at the center of the head. The effects of the irregular shape defect and presence of the control-rod penetrations were not included. The ABAQUS commercial finite element analysis software was used with four-noded axisymmetric elements. Figure 6 shows the detailed finite element mesh.

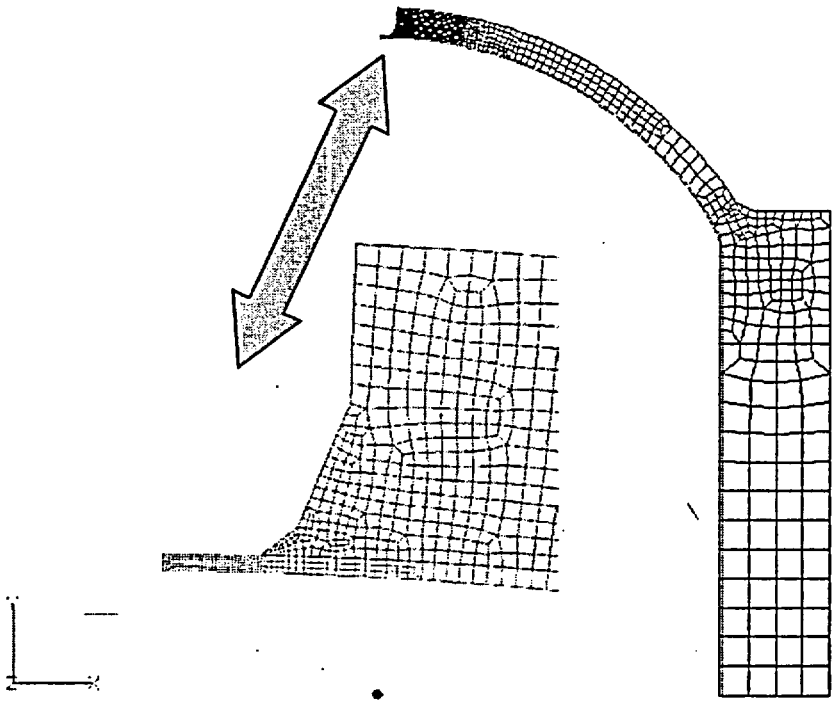

Figure 6 Axisymmetric finite element mesh for the Davis-Besse head

The dimensions of the Davis-Besse head used in these analyses were taken from detailed drawing supplied with the FirstEnergy's submittal to NRC bulletin 2001-01 (Docket Number 50-346). Four or five elements were used through the cladding thickness at the center location and 6 to 7 elements at the transition point from the cladding to the RPV head. The cladding thickness and the diameter of the corrosion hole were defined as variables. Large-strain analyses were conducted assuming incremental plasticity with isotropic hardening in the constitutive relationship. The detailed uniaxial stress-strain curve used for the cladding came from Framatome in response to a request from Emc^2, ORNL, and the NRC as is described in the previous section. An elastic-plastic stress-strain curve was used for the head material, but the stresses in the head material are generally elastic and have very little effect on the strains in the center of the cladding.

The stress-free temperature was 605F in these calculations. SIA used a stress-free temperature of room temperature, whereas the stress free temperature may be closer to 1,100F (the stress-relief temperature of the head after the cladding is put on). The cladding had a higher coefficient of thermal expansion than the low alloy steel head. Hence, using the stress-free temperature of 70F and taking the head to 605F produces a compressive stress in the cladding (SIA approach), our analysis was stress-free, but the real

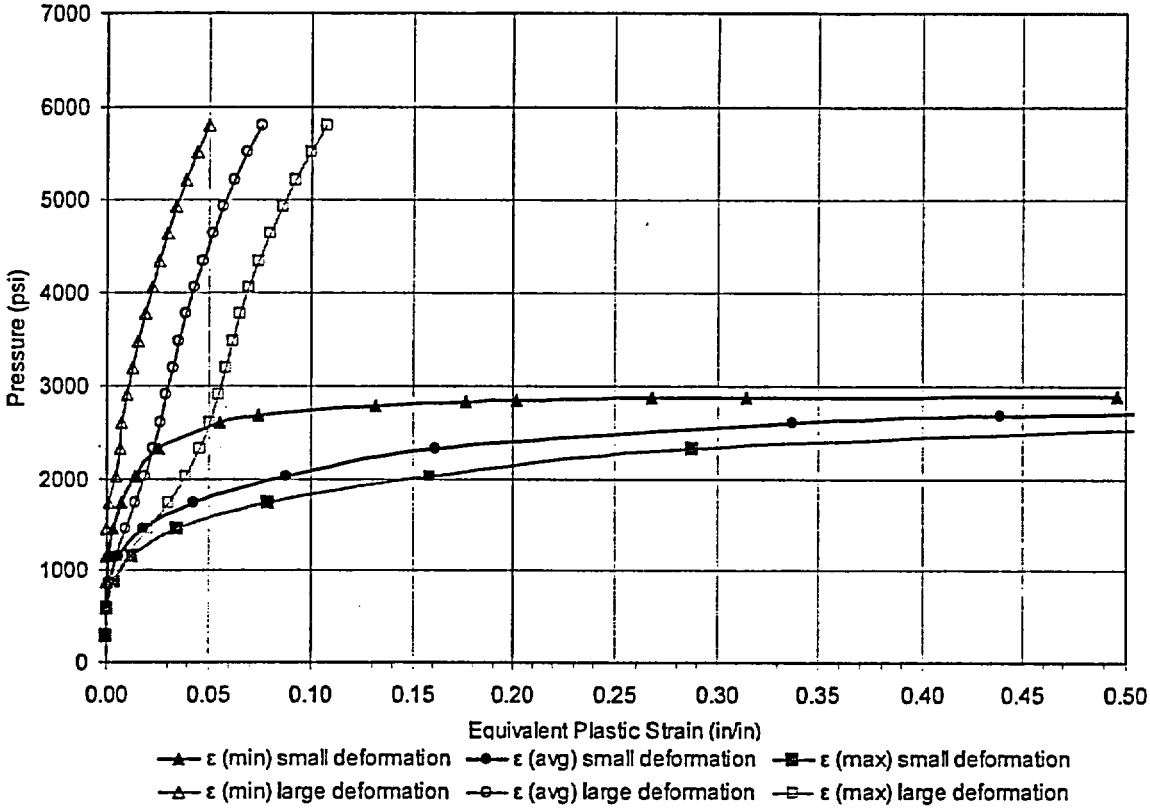

Figure 7 Plot of equivalent plastic strain at center of cladding versus internal pressure for both small-deformation and large-deformation analyses for a 6-inch diameter corrosion area and a cladding thickness of 0.297 inch

RESULTS OF PARAMETRIC STUDY SHOWING "FAILURE PRESSURE" VERSUS CORRODED AREA

In order to simplify the numerous pressure versus strain plots that are given in Appendix A, the pressure as a function of corrosion diameter corresponding to the maximum, the minimum, and the average strain in the cladding layer for both the 5.5% and 11.2% strain levels were determined. Recall that the 5.5% strain criterion was determined by considering the effect of biaxial loading on the stress-strain curve up to the same uniaxial ultimate stress value. No efforts could be made at this time to estimate if necking would occur at a lower stress value due to the higher triaxial stress conditions in the actual structure than in a uniaxial tensile test. Experimental data or more detailed analyses are needed to make that determination. Results of the critical strain being reached either in the center of the cladding or at the edge were investigated. First the center cladding location results are given in detail and reduced to the key figure. For the edge location, the detailed plots are given in Appendix A, and only the key figure is given. A comparison of the two plots for determining a calculated "failure pressure" is given afterwards.

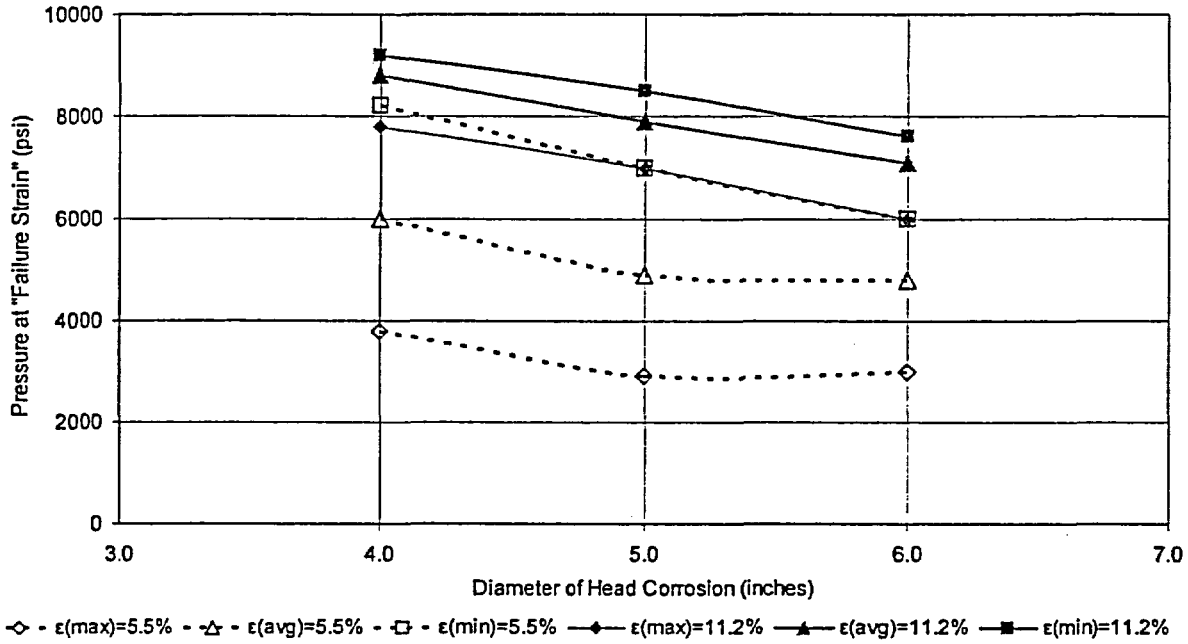

Figure 9 Corrosion diameter versus "failure pressure" for critical strain at center of cladding for cladding thickness of 0.297 inch

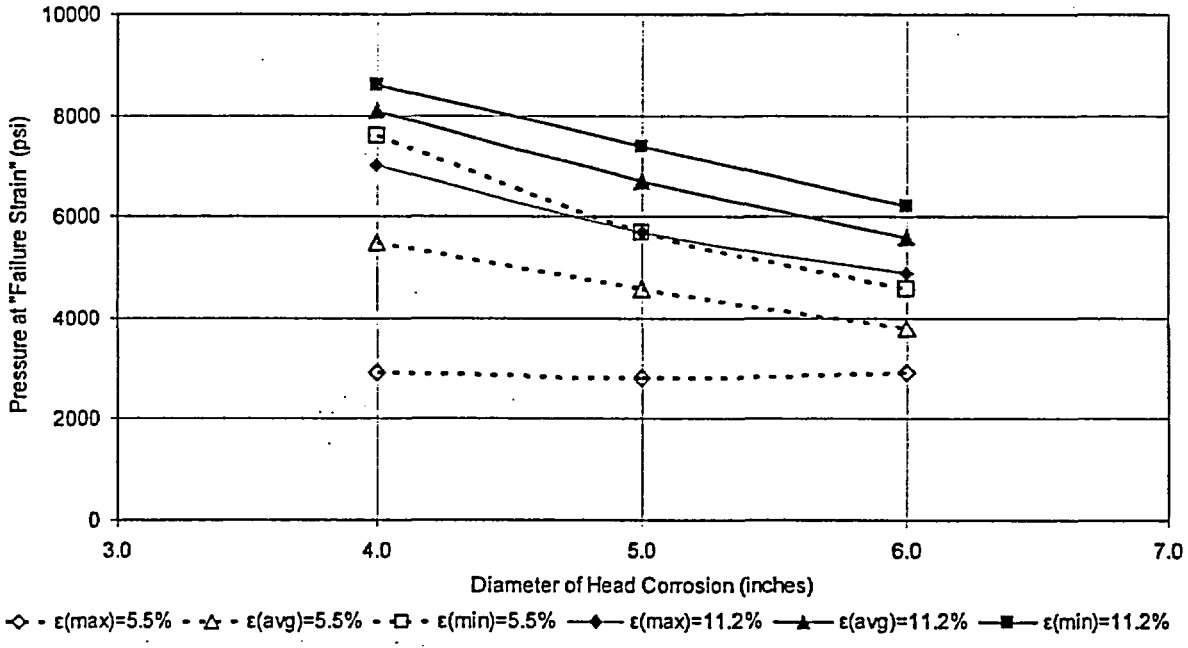

Figure 10 Corrosion diameter versus "failure pressure" for critical strain at center of cladding for cladding thickness of 0.240 inch

Another way to assess this data is to plot the "failure pressure" versus cladding thickness for a given diameter of corrosion. One plot of this type is shown in Figure 13 for illustration purposes.

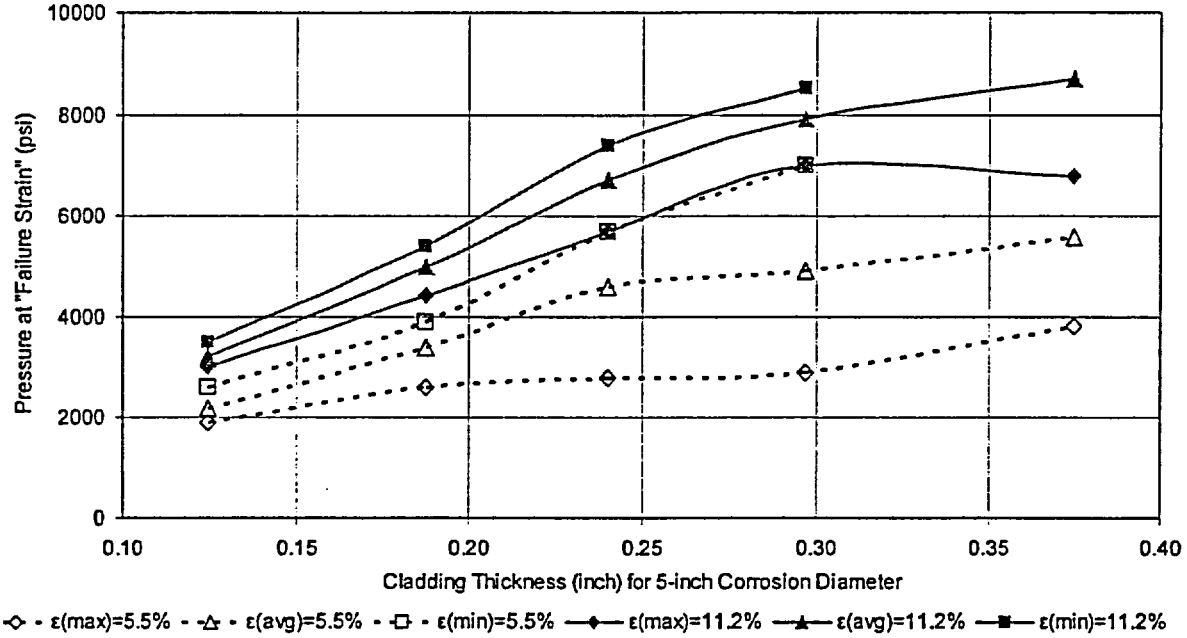

Figure 13 Cladding thickness versus "failure pressure" for critical strain at center of cladding for 5-inch diameter corrosion area

Values from Figure 9 through Figure 12 have been combined by normalizing the corrosion diameter with respect to the ligament thickness and plotting the results versus "failure pressure" for having the strain in the center of the cladding. Plots of pressure versus D/t are shown in Figure 14 and Figure 15 for the critical strains of 5.5% and 11.2%, respectively. The three different strain gradient criteria are shown in each figure. These figures show that the data from the pressure-versus-diameter plots for each thickness collapse to a single curve for a given failure criterion. The first occurrence curves are believed to give too low of "failure pressure", whereas the average strain curves are believed to give a best estimate of the expected failure pressure. Hence, Figure 14 and Figure 15 can be used to calculate the "failure pressure" for a significant range of corrosion diameters and thicknesses of interest.

Figure 16 shows a comparison of the 5.5% average-failure-strain criterion (Emc^2 best-estimate failure criterion) to the 11.2% minimum-failure-strain criterion (SIA criterion).

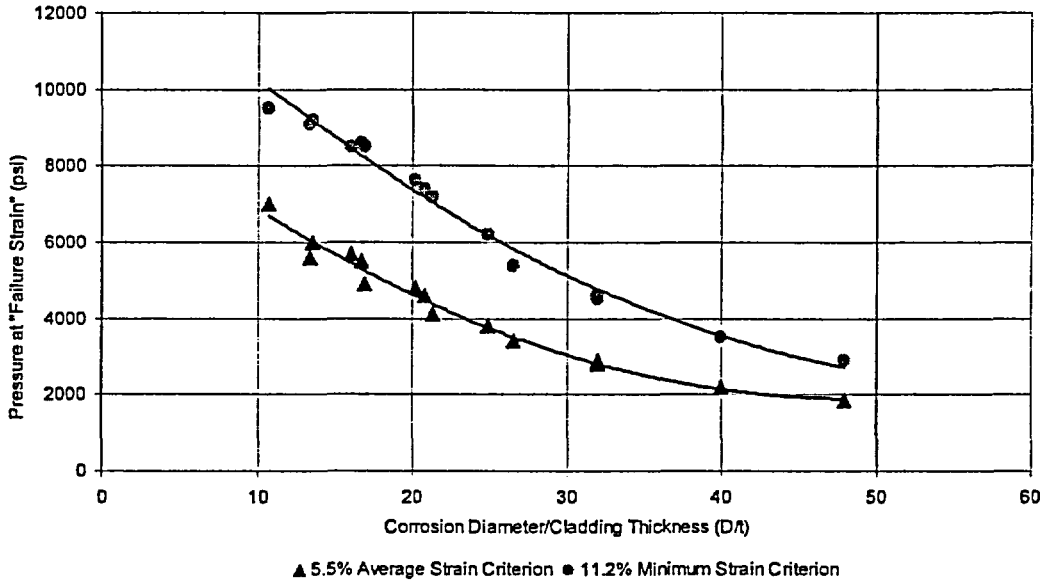

Figure 16 Plot of D/t versus pressure for comparing the 5.5% average failure strain criterion to the 11.2% minimum failure strain criterion at center of cladding

Figure 17 shows the ratio of the failure pressures for the 11.2% minimum strain criterion at the center of the cladding (SIA failure criterion) to the 5.5% average strain criterion (Emc^2 best-estimate failure criterion) as a function of corrosion diameter to cladding thickness, D/t. The figure shows that the failure pressure using the 11.2% minimum strain criterion exceeds that of the 5.5% average strain criterion by approximately 60% over the range of D/t investigated.

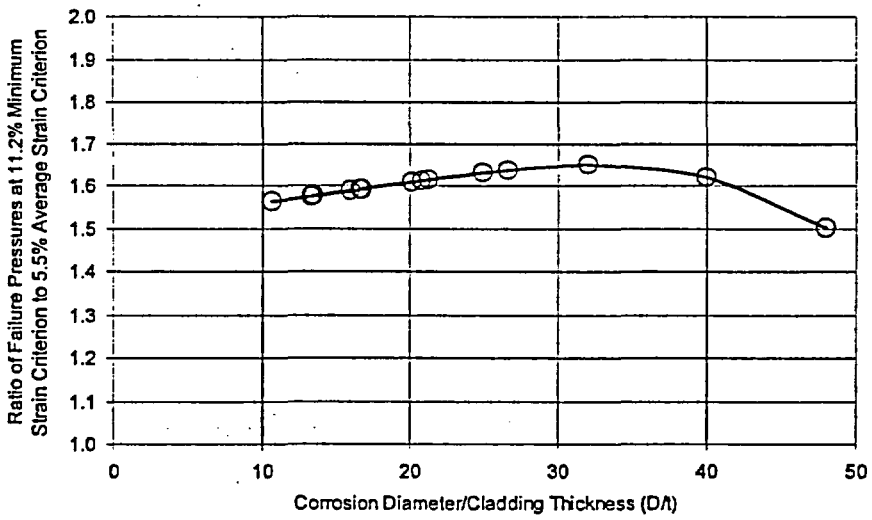

Figure 17 Ratio of the "failure pressures" from 11.2% minimum strain criterion used by SIA to the Emc^2 best-estimate 5.5% average strain criterion as a function of corrosion diameter to cladding thickness (D/t) at center of cladding

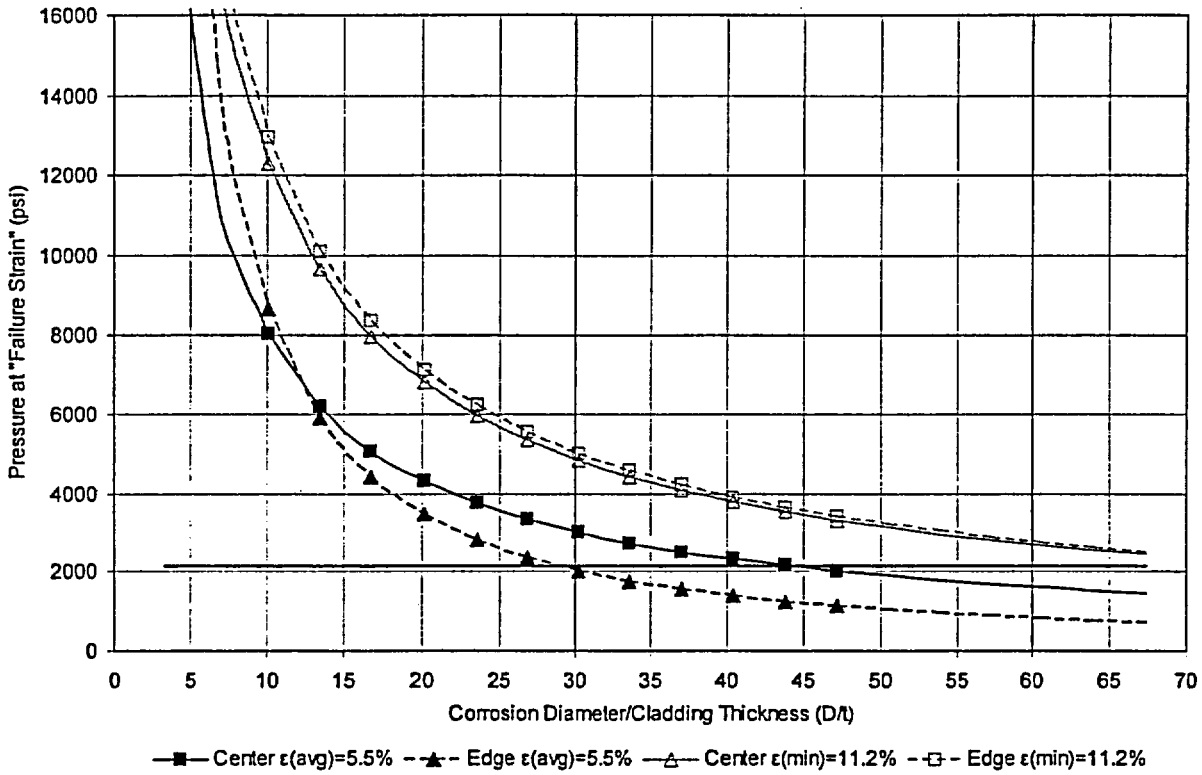

Figure 19 Comparison of "failure pressures" versus D/t for center and edge locations

Calculated Margins

To determine the margins on either the failure pressure or the margin on the hole diameter, it is first necessary to characterize the corrosion area in terms of an equivalent diameter. Figure 20 shows the remaining thickness measured on the RPV head between Nozzles 3 and 11. These measurements were taken at a spacing of approximately one square inch by Davis-Besse and their contractors. While these were preliminary measurements, the figure shows that the minimum thickness of 0.240 inch was measured at one location. In addition, there is a region between the nozzle openings where the thickness is less than 0.300 inch over an irregular area. The longest continuous segment in which the cladding thickness does not exceed 0.300 inch is approximately 6.7 inches, as shown by the solid line, or 7.6 inches as shown by the dashed line where only one reading was greater than 0.300 inch in Figure 20.

Margins on Failure Pressures

The fit through the finite element results shown in Figure 19 was used to make a plot of the bounding failure pressure versus hole diameter for a cladding thickness of 0.297 inch. The results are shown in Figure 21 for corrosion defect diameters up to 20 inches. The symbols in Figure 21 indicate were FE results were available. The solid line beyond the symbols is an extrapolated curve-fit equation. A nominal operating pressure of 2,155 psi is also indicated in the figure.

Assuming that the shape of the corrosion defect has less affect on the failure pressure than the largest meridianal dimension (from gas pipeline corrosion experience), then using the approximate meridianal dimensions of 6.7 to 7.6 inches (from Figure 20) gives a "best-estimate failure pressure" range of 3,000 to 2,300 psig, respectively. This gives a margin on the operating pressure of 1.39 to 1.07, respectively. Both of these failure predictions are for the edge location, where the actual geometry used is not well known at this time.

Using these same dimensions with the minimum-strain failure criterion with 11.2% critical strain (SIA criterion), the calculated failure pressure would be about 6,300 to 5,700 psig, respectively. This gives a margin of 2.92 to 2.65, respectively.

The ratio of the failure pressures from the two criteria is roughly the factor of 2.2. This is greater than the 1.6 value from Figure 17 since the 5.5% strain criterion has the critical location at the edge of the hole not at the center.

Margins on Corrosion Cavity Diameter

Another estimate that could be made from Figure 21 is the size of the corrosion area that could cause failure at the normal operating pressure. Using the average strain criterion with 5.5-percent critical strain gives a meridianal length (diameter from Figure 21) of approximately 8.5 inches, or 0.9 to 1.8 inches of additional corrosion length. Using the SIA minimum-strain failure criterion with 11.2-percent strain gives a meridianal length of approximately 23 inches (extrapolated from Figure 21), or 15.3 to 16.3 inches of additional corrosion for failure at the operating pressure.

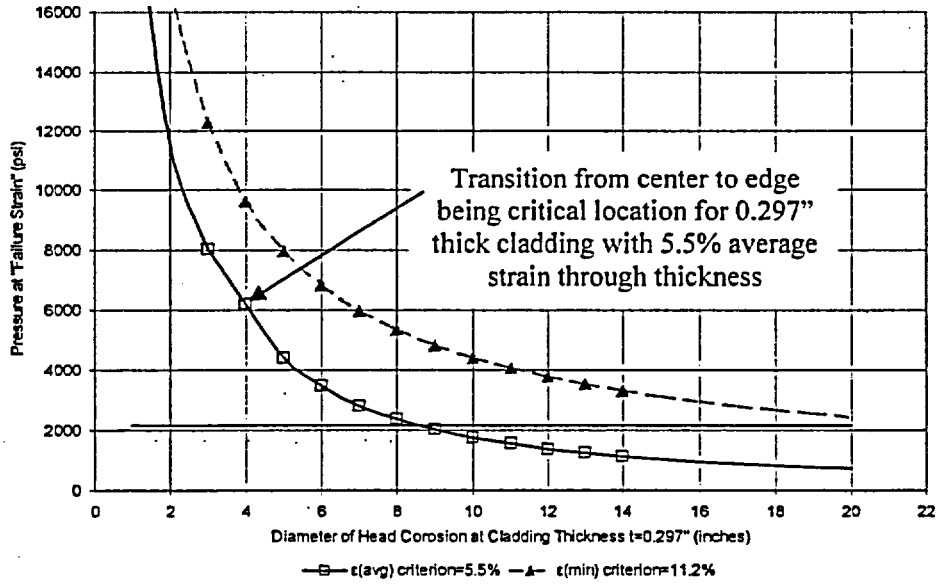

Figure 21 Extrapolated curve-fit of FE values for a cladding thickness of 0.297 inch

The relatively good agreement between the Emc^2 and modified SIA results (when using the same failure criterion) predicted the critical location as being at the edge of the cladding region. The higher preliminary ORNL results have the failure at the center of the cladding. Additional refinement of the mesh in the ORNL analysis is underway to explore this.

CONCLUSIONS

The efforts conducted in this report involved making a best-estimate evaluation to determine the margins on the calculated "failure pressure" to operating pressure and how much additional corrosion might be needed to cause failure at the operating pressure for the Davis-Besse RPV head corrosion case. The conclusions from this investigation were:

1. The uniaxial stress-strain curve at 600F supplied by Framatome from the *Nuclear Systems Materials Handbook* was compared to stress-strain curves for TP308 weld metal at 550F from the PIFRAC database and was found to be more representative of the average stress-strain curve from the PIFRAC database rather than a minimum value. The material documented in the PIFRAC database was not stress relieved, and it is not known if the *Nuclear Systems Materials Handbook* material was stress relieved. The cladding on the head was stress relieved. Stress relieving may slightly reduce the stress-strain curve.

2. The uniaxial stress-strain curve can be used to calculate the strain at the same ultimate stress value for biaxial loading. This involves a relatively fundamental use of Hook's Law, Von Mises equation, and the Distortion Energy Theorem. The resulting strain under biaxial loading was about half of the uniaxial strain for the TP308 weld metal; i.e., 5.5-percent strain, rather than 11.2 percent strain. This result is consistent with engineering judgment for several metallurgist, and university professors that deal with metal-forming-limit diagrams for biaxial loading in the automotive and shipbuilding industries. An analysis by McClintock on failure stress for a sphere under pressure loading (pure biaxial membrane loading) gave a similar trend for pure 1:1 biaxial loading.

3. Fifteen axisymmetric finite element analyses were conducted with large-strain assumptions. The pressures corresponding to the equivalent strains were calculated for a variety of cladding thicknesses and cavity diameters. The strains varied through the thickness of the cladding, so pressures corresponding to three possible failure criteria were calculated:
    a. The pressure when the cladding strain was first reached the critical strain,
    b. The pressure when the average strain through the thickness of the cladding reached the critical strain, and
    c. The pressure when the strain in the entire thickness of the cladding exceeded the critical strain.

    It was felt that Criterion (a) would be too conservative, Criterion (b) was a reasonable best estimate in the absence of experimental data or further detailed analyses, and Criterion (c) would overestimate the failure pressure.

4. The location of the "critical strain" could be at either the central region of the cladding or along the edge. The precise edge support geometry (how the head corroded close to the cladding) is not well known at this time, so a straight segment approximation of the transition was used in the models. With this edge condition, the critical strain location was at the edge of the clad-only region in our analysis. This was consistent with the SIA results.

12. More detailed analyses for the ORNL efforts will be helpful in determining the margins estimated from the plastic displacement or bowing in the cladding that was measured in the Davis-Besse head once further refinement of the mesh is made.

13. The accuracy of the "failure criterion" may require some experimental data to determine the biaxial strain limit of the cladding material at the operating temperature. Alternatively, a FE analysis using Gurson elements in ABAQUS could be conducted if the proper parameters for the Gurson element can be determined for the cladding material (inclusion size and distribution [f_0 and D values from the Tvergaard and Hutchinson approach[9]]). Test data exist where those values could be independently determined and then applied to the unflawed (or even a flawed) cladding analysis.

14. It is recommended that once the corroded region is cut from the head and sent for evaluation, the geometry of the transition from the cladding layer to the outside surface of the RPV head be determined. A silicon mold of the cladding surface could be made to determine the variability of the thickness.

[9] C. F. Shih, L. Xian, and J. Hutchinson, "Validity Limits in J-Resistance Curve Determination – A Computational Approach to Ductile Crack Growth under Large-Scale Yielding Conditions," NUREG/CR-6264, Vol. 2, February 1995.

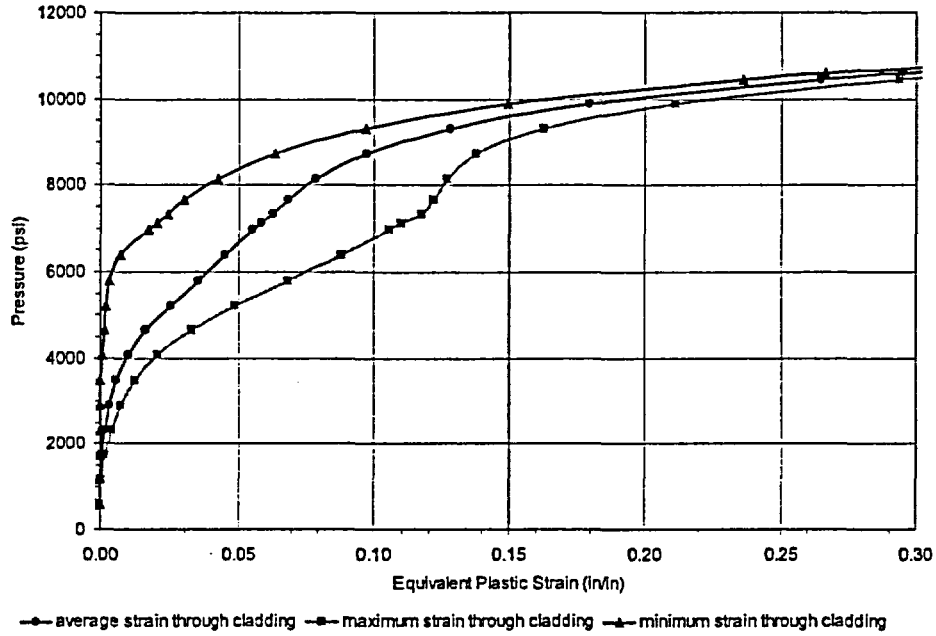

Figure A-1 Equivalent plastic strain versus pressure at the center for corrosion diameter of 4 inches and cladding thickness of 0.375 inch

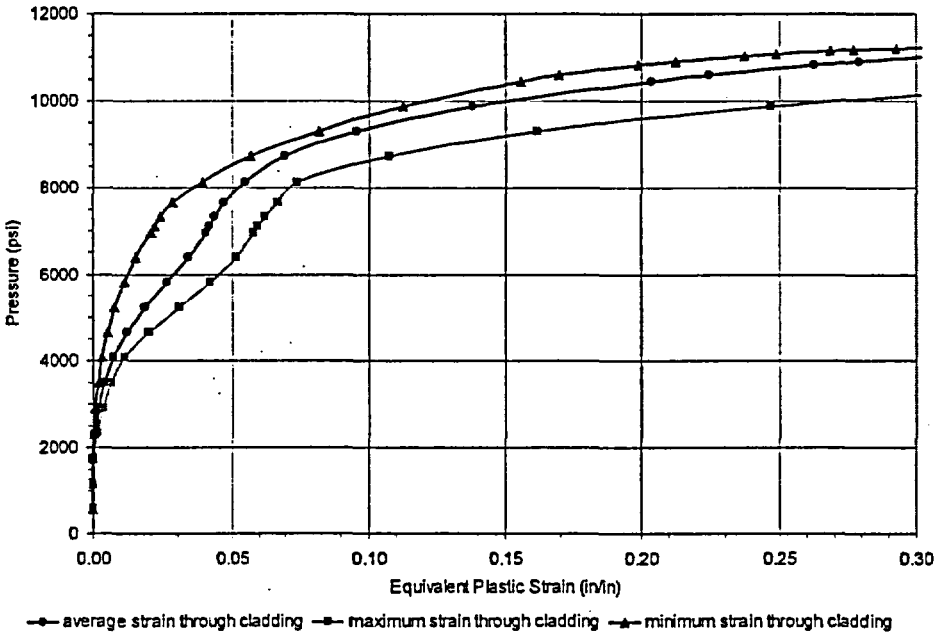

Figure A-2 Equivalent plastic strain versus pressure at the edge for corrosion diameter of 4 inches and cladding thickness of 0.375 inch

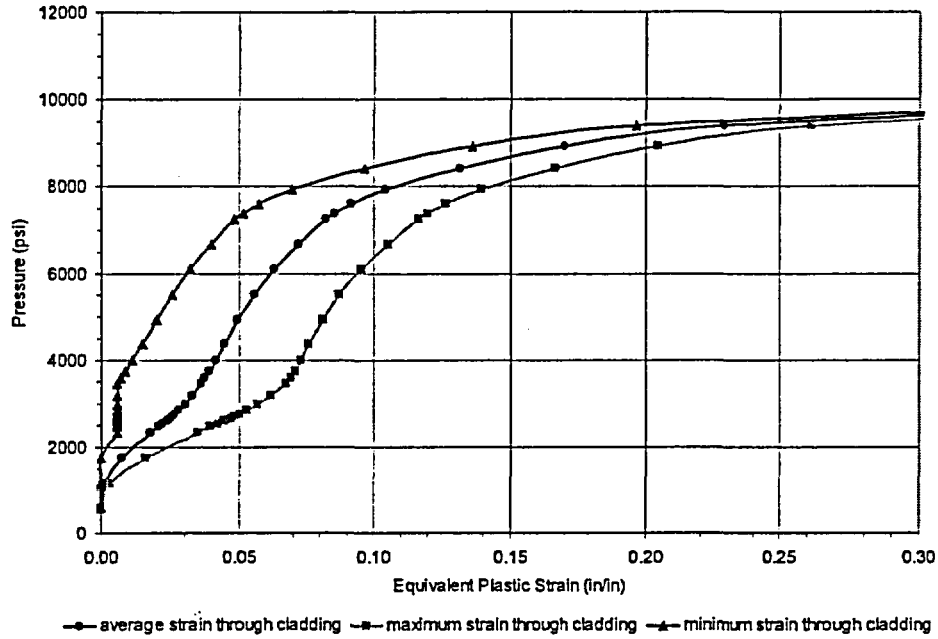

Figure A-5 Equivalent plastic strain versus pressure at the center for corrosion diameter of 4 inches and cladding thickness of 0.240 inch

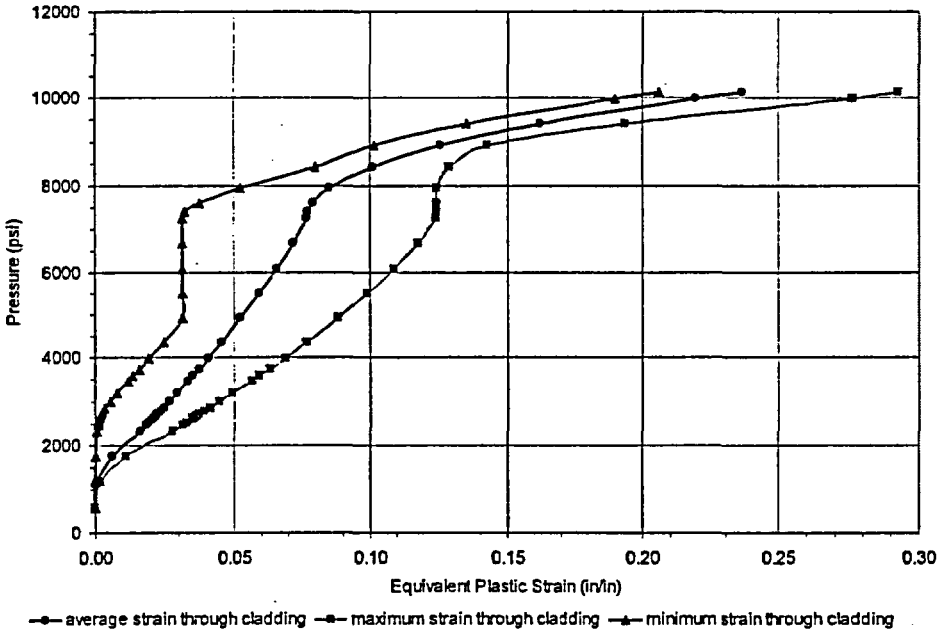

Figure A-6 Equivalent plastic strain versus pressure at the edge for corrosion diameter of 4 inches and cladding thickness of 0.240 inch

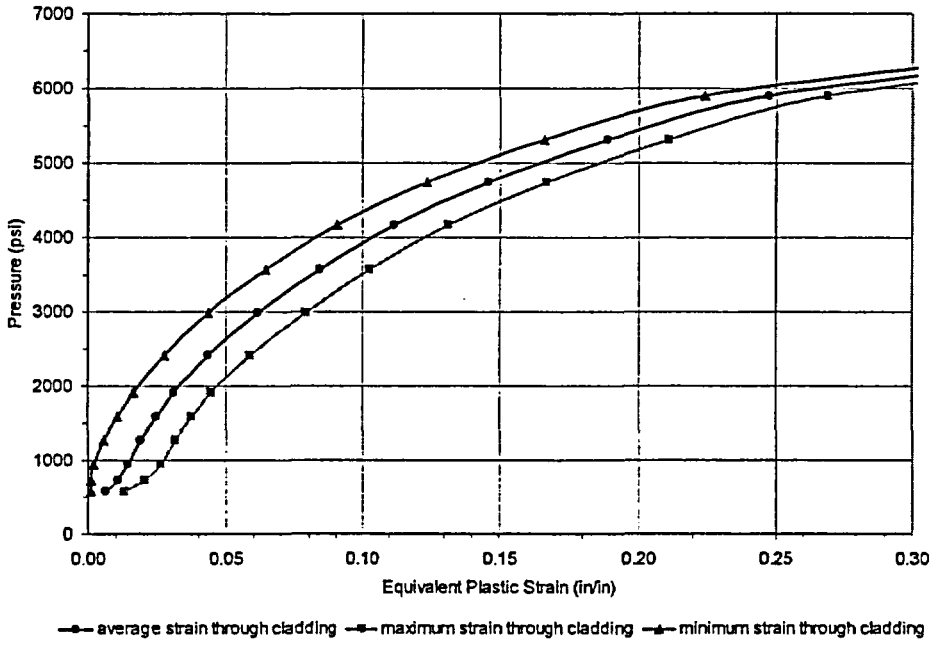

Figure A-9 Equivalent plastic strain versus pressure at the center for corrosion diameter of 4 inches and cladding thickness of 0.125 inch

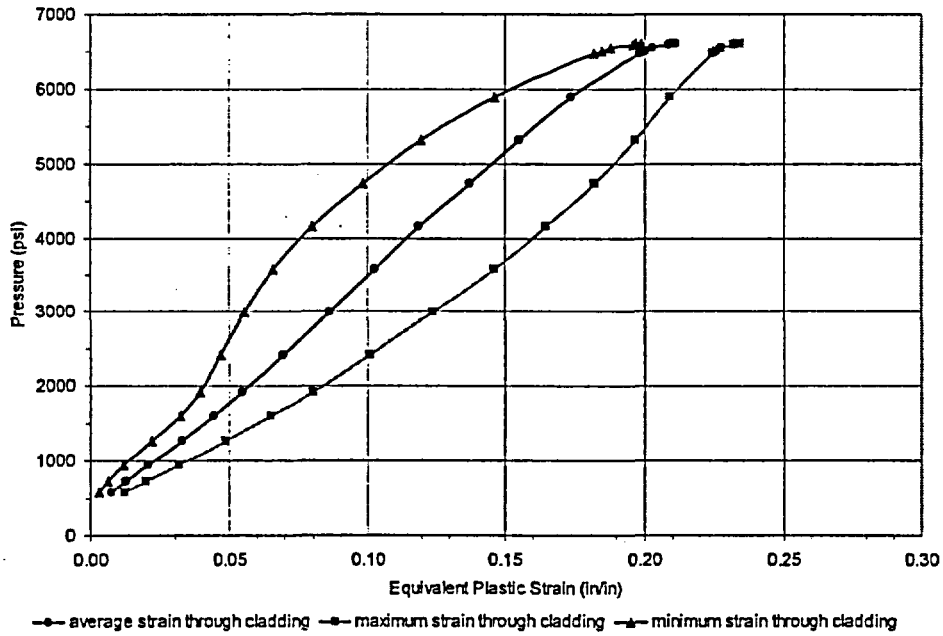

Figure A-10 Equivalent plastic strain versus pressure at the edge for corrosion diameter of 4 inches and cladding thickness of 0.125 inch

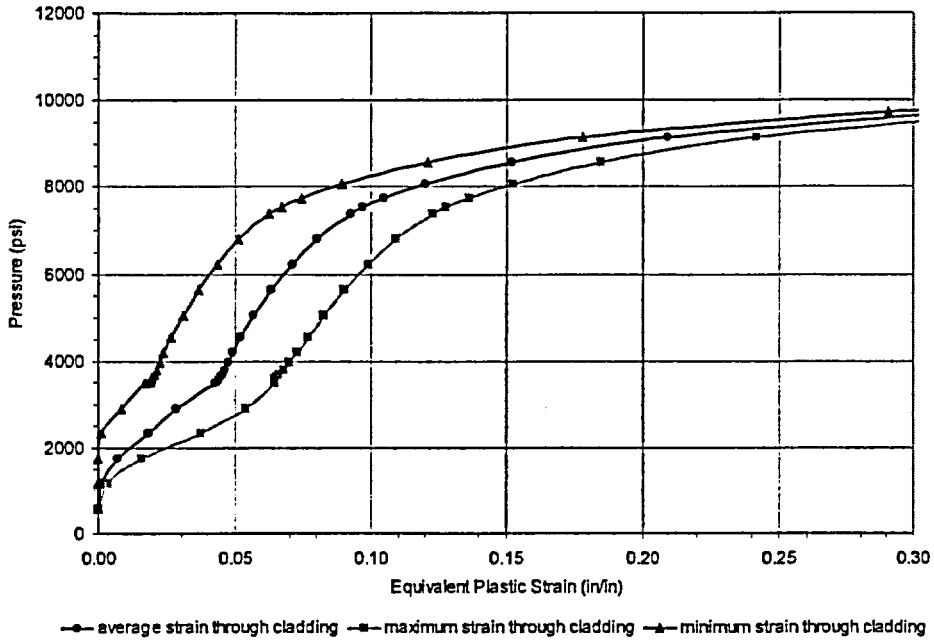

Figure A-13 Equivalent plastic strain versus pressure at the center for corrosion diameter of 5 inches and cladding thickness of 0.297 inch

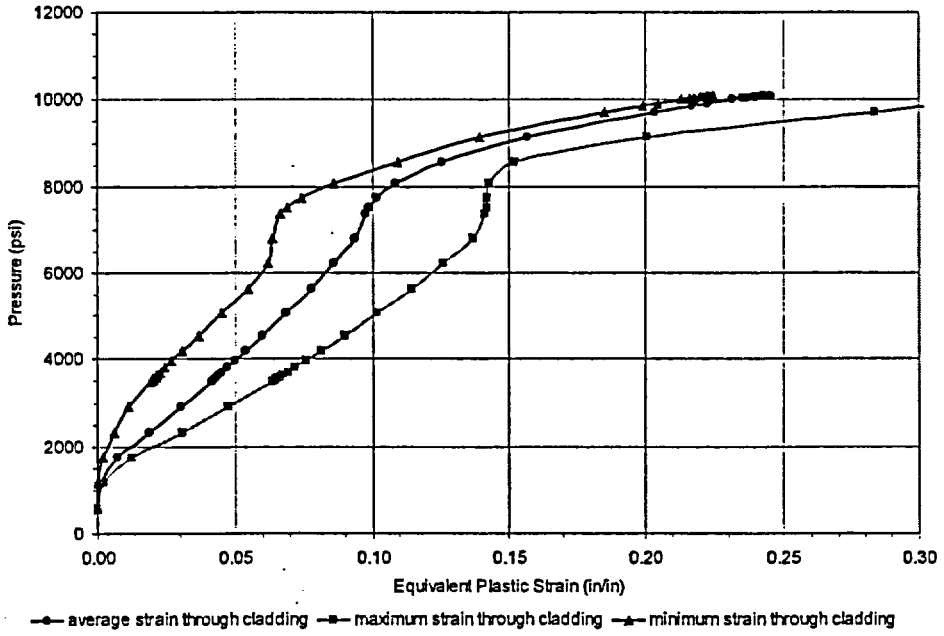

Figure A-14 Equivalent plastic strain versus pressure at the edge for corrosion diameter of 5 inches and cladding thickness of 0.297 inch

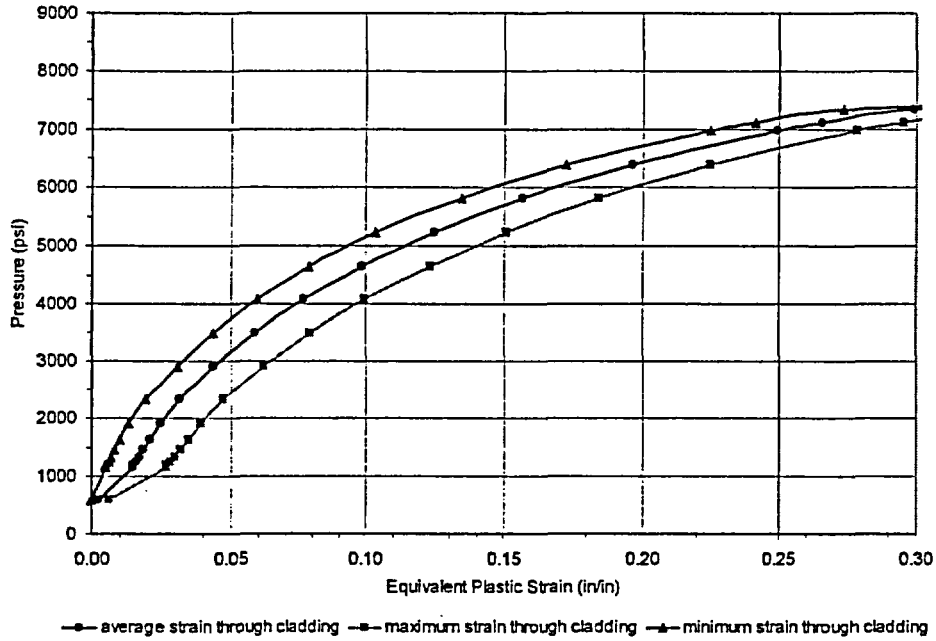

Figure A-17 Equivalent plastic strain versus pressure at the center for corrosion diameter of 5 inches and cladding thickness of 0.188 inch

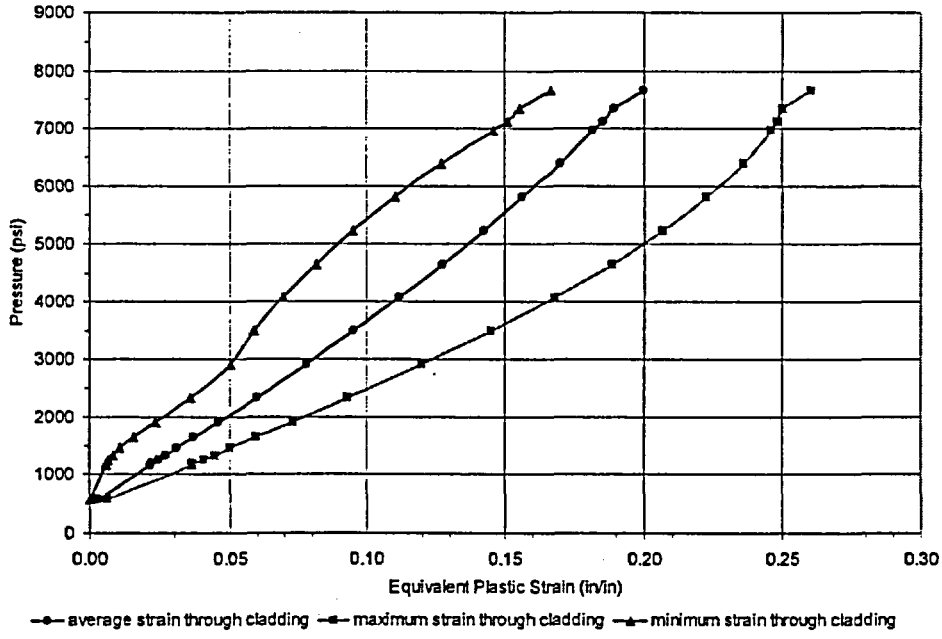

Figure A-18 Equivalent plastic strain versus pressure at the edge for corrosion diameter of 5 inches and cladding thickness of 0.188 inch

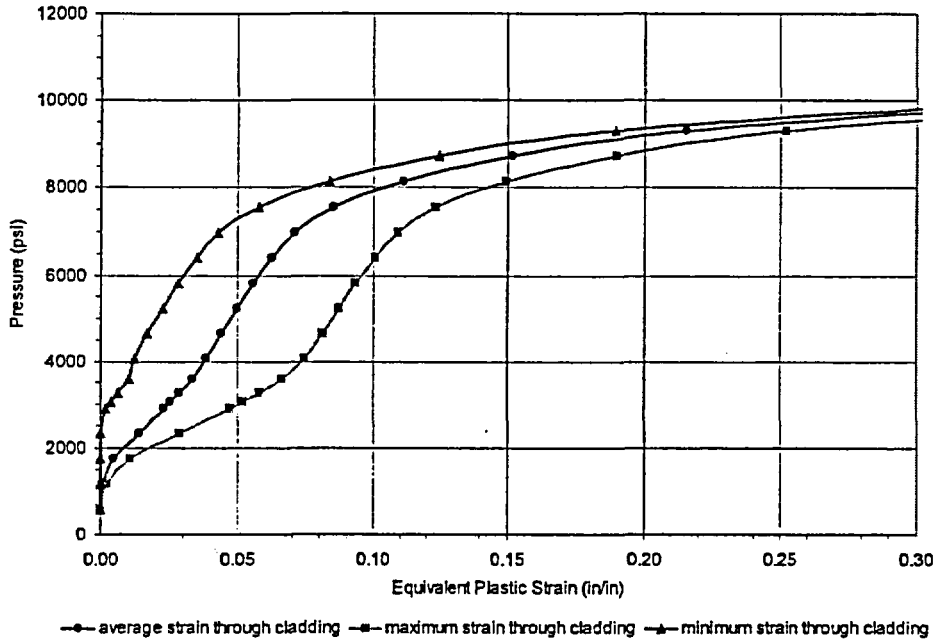

Figure A-21 Equivalent plastic strain versus pressure at the center for corrosion diameter of 6 inches and cladding thickness of 0.375 inch

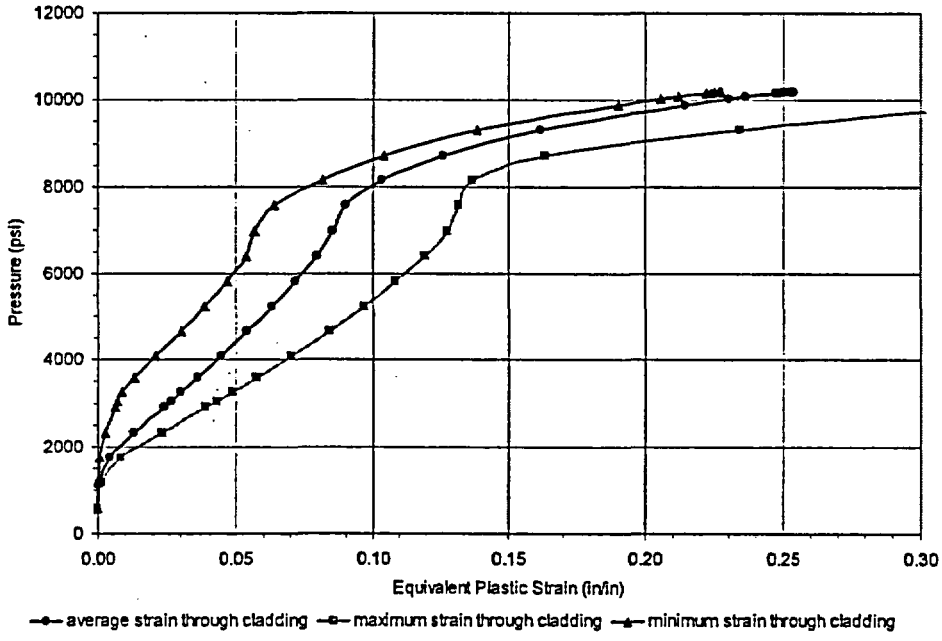

Figure A-22 Equivalent plastic strain versus pressure at the edge for corrosion diameter of 6 inches and cladding thickness of 0.375 inch

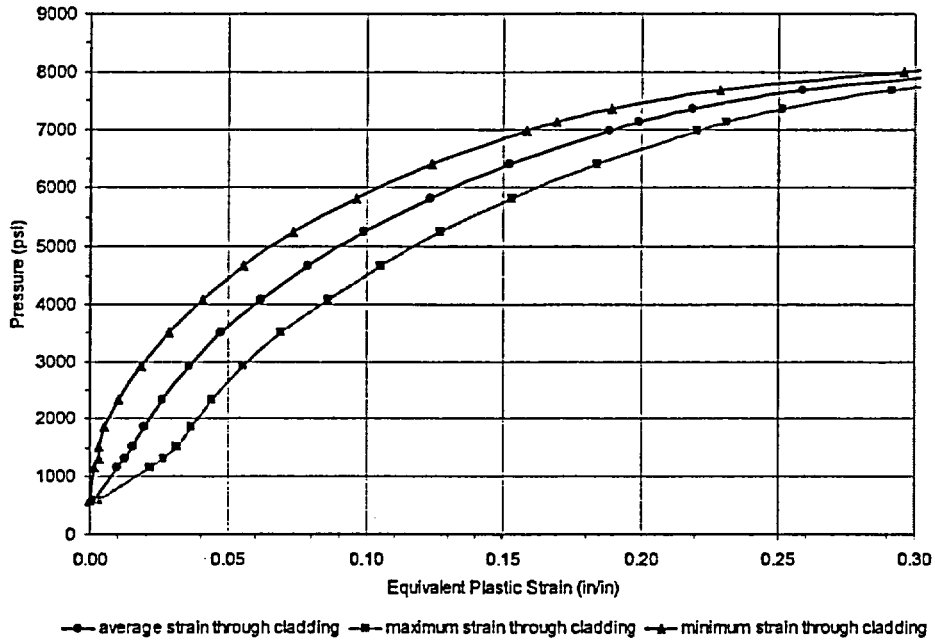

Figure A-25 Equivalent plastic strain versus pressure at the center for corrosion diameter of 6 inches and cladding thickness of 0.240 inch

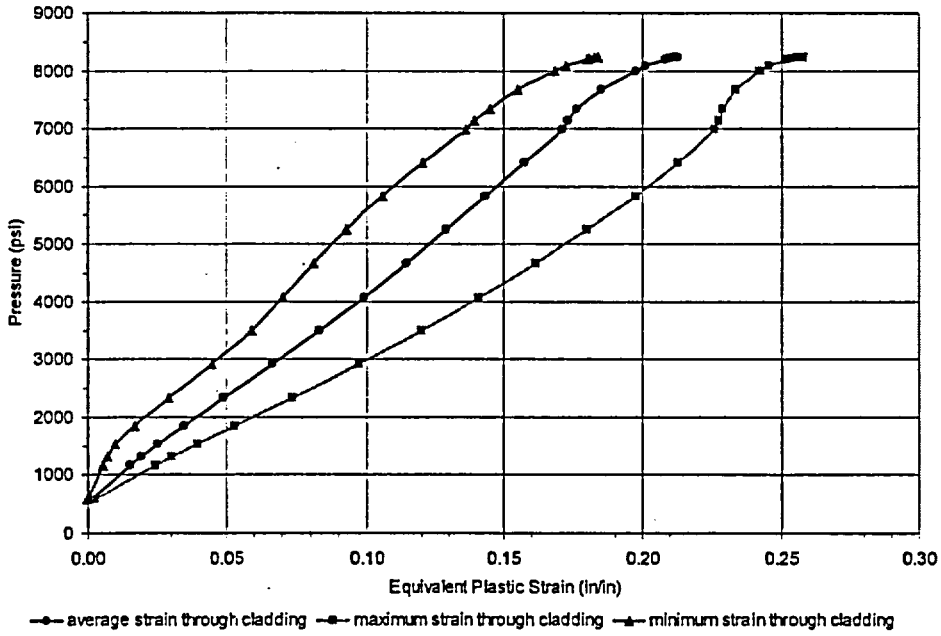

Figure A-26 Equivalent plastic strain versus pressure at the edge for corrosion diameter of 6 inches and cladding thickness of 0.240 inch

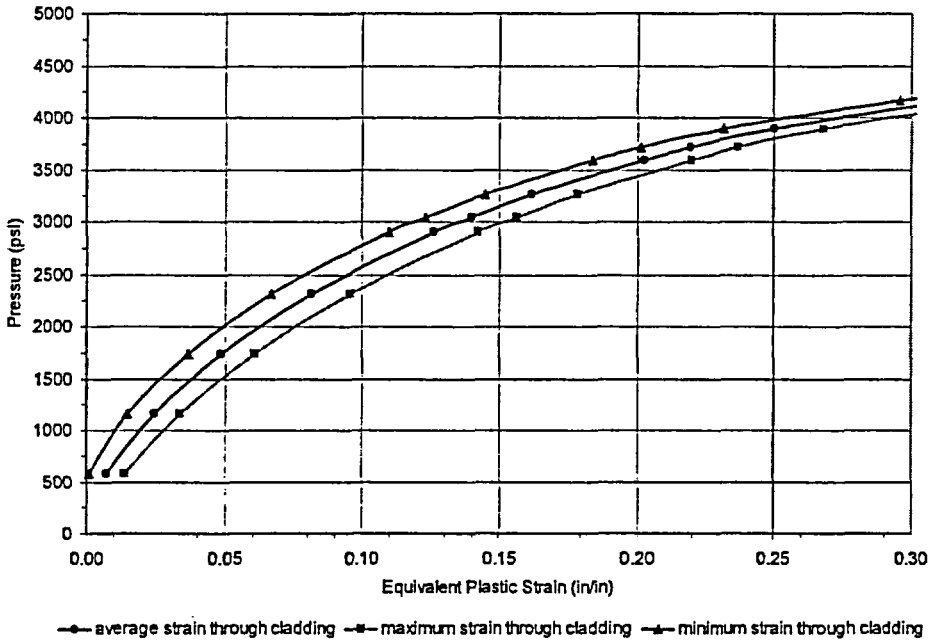

Figure A-29 Equivalent plastic strain versus pressure at the center for corrosion diameter of 6 inches and cladding thickness of 0.125 inch

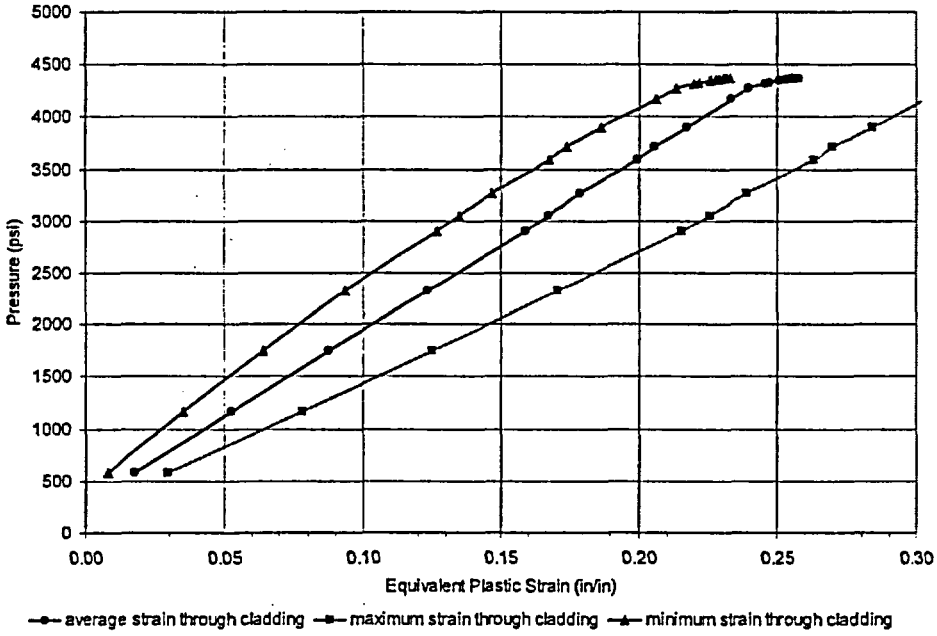

Figure A-30 Equivalent plastic strain versus pressure at the edge for corrosion diameter of 6 inches and cladding thickness of 0.125 inch

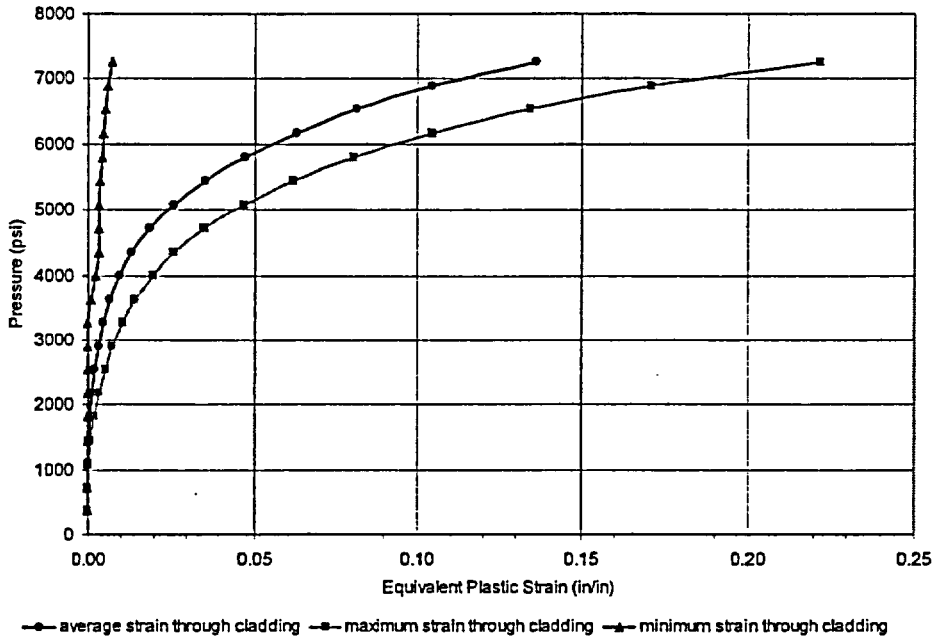

Figure B 1 Equivalent plastic strain versus pressure for corrosion diameter of 4 inches and cladding thickness of 0.375 inch

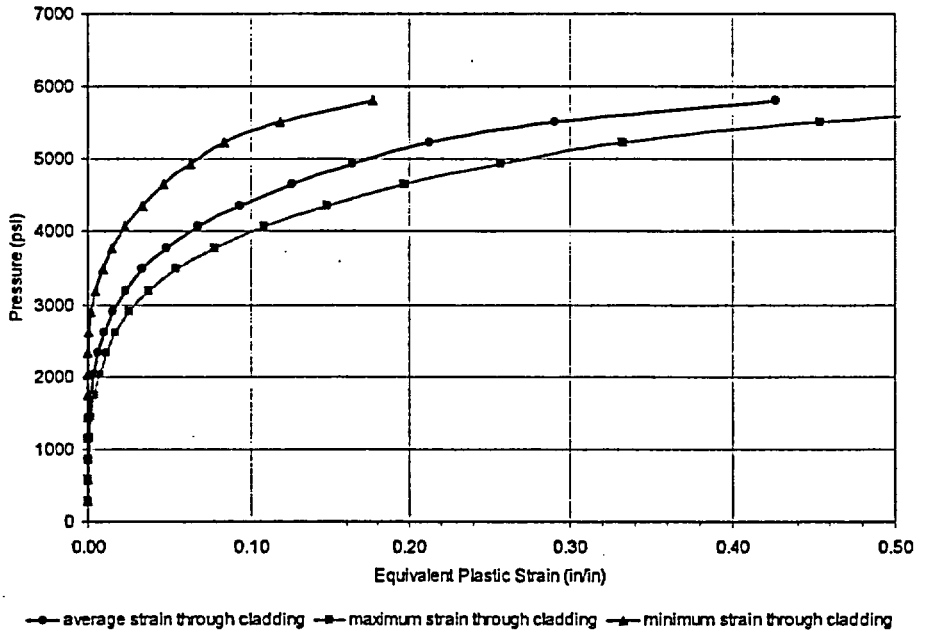

Figure B 2 Equivalent plastic strain versus pressure for corrosion diameter of 4 inches and cladding thickness of 0.297 inch

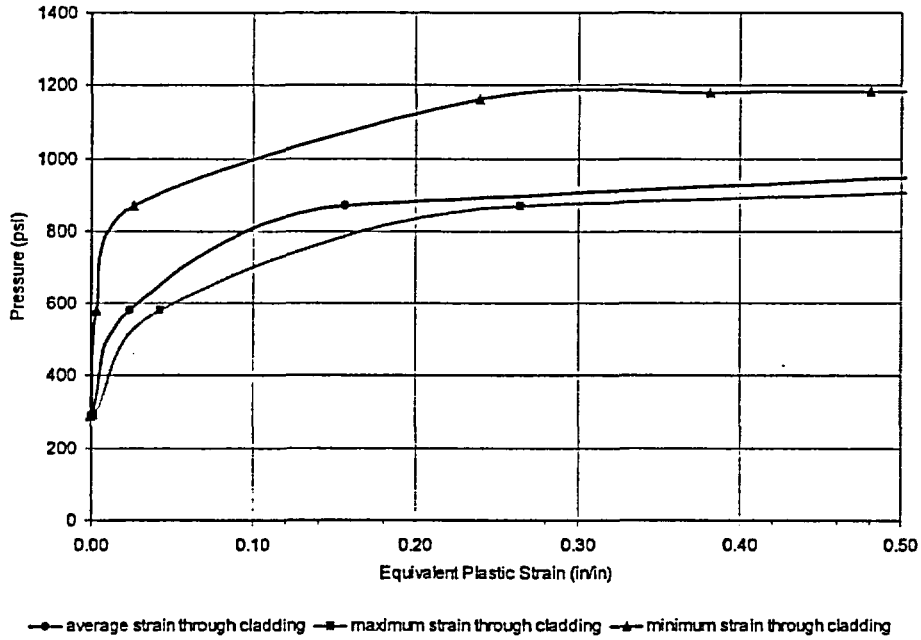

Figure B 5 Equivalent plastic strain versus pressure for corrosion diameter of 4 inches and cladding thickness of 0.125 inch

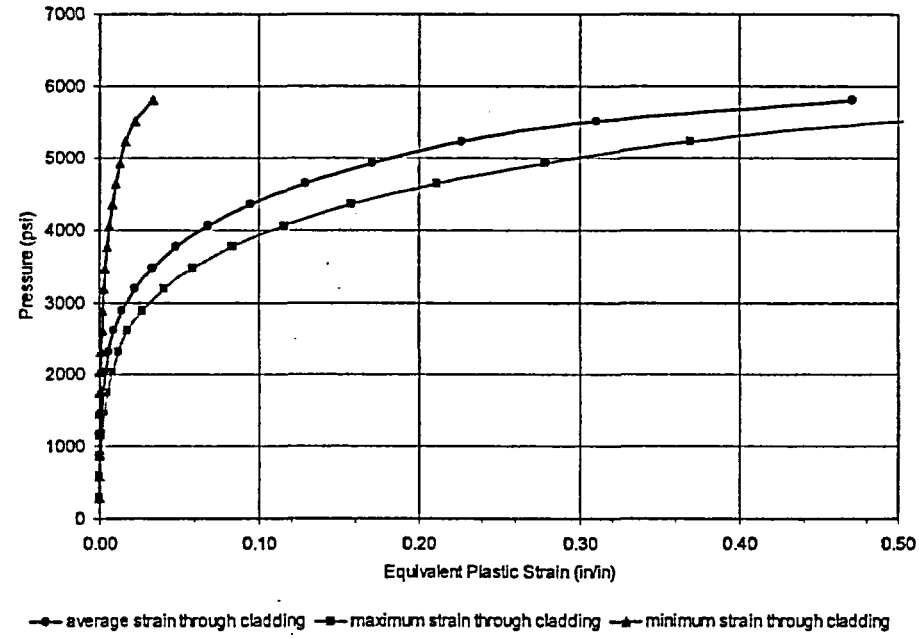

Figure B 6 Equivalent plastic strain versus pressure for corrosion diameter of 5 inches and cladding thickness of 0.375 inch

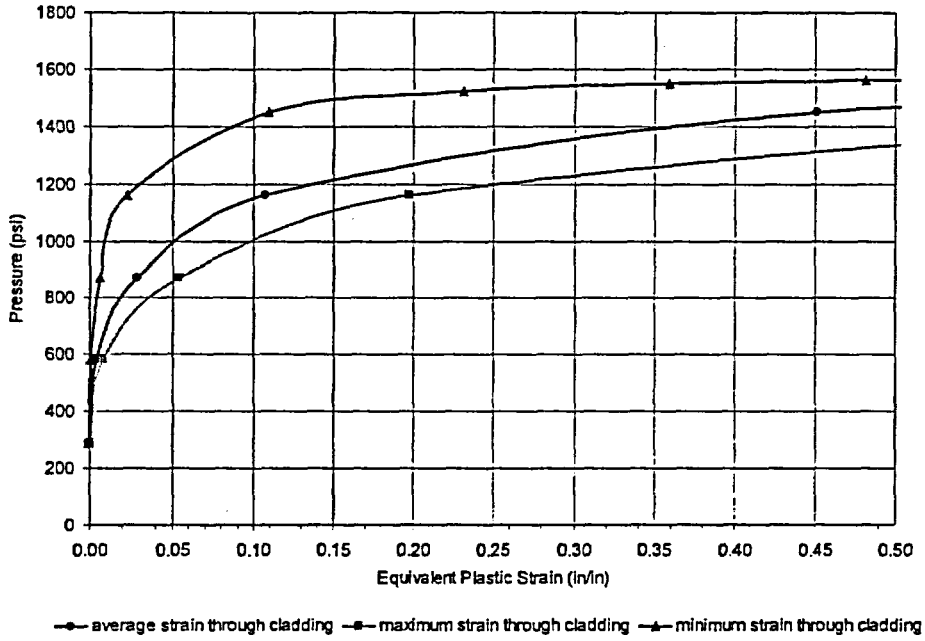

Figure B 9 Equivalent plastic strain versus pressure for corrosion diameter of 5 inches and cladding thickness of 0.188 inch

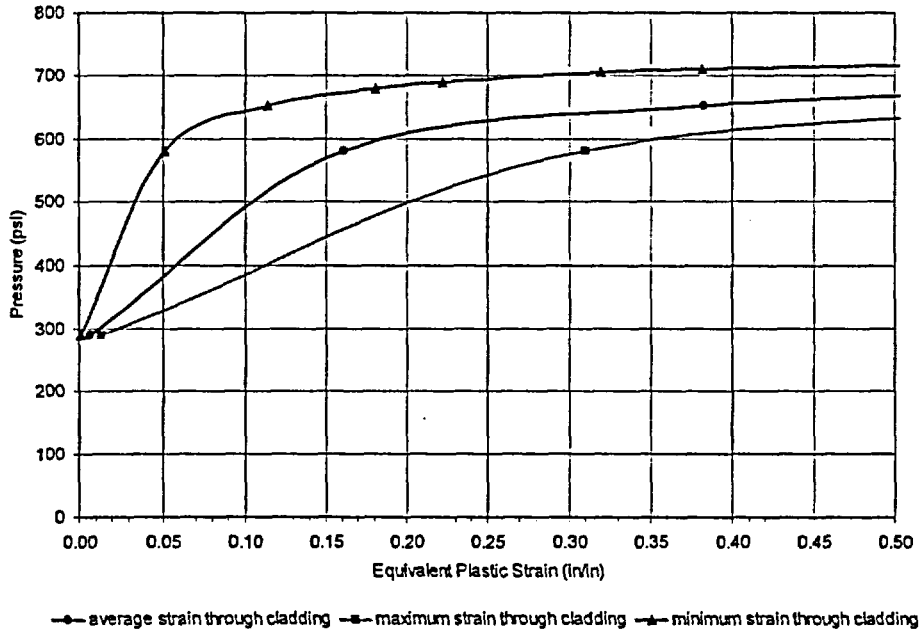

Figure B 10 Equivalent plastic strain versus pressure for corrosion diameter of 5 inches and cladding thickness of 0.125 inch

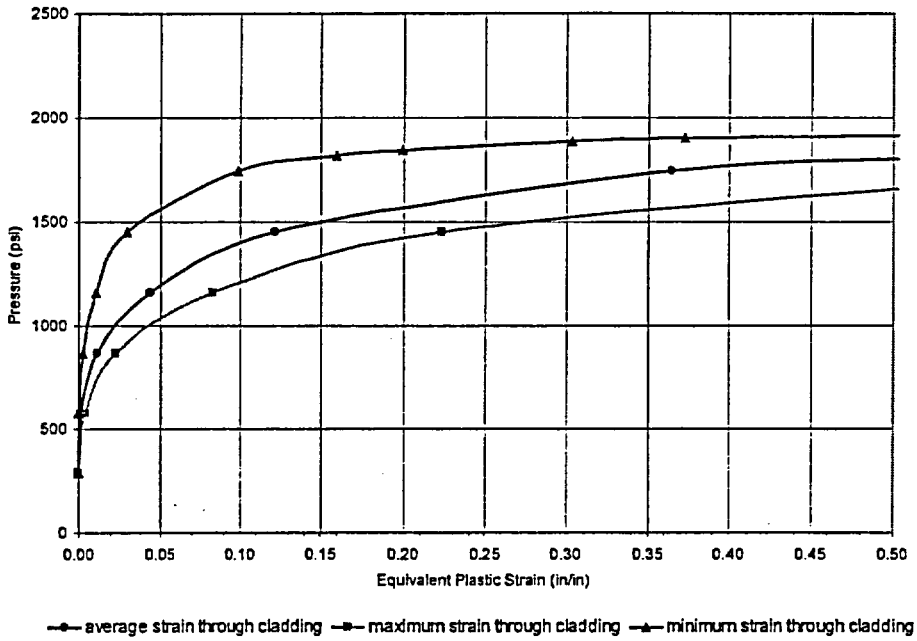

Figure B 13 Equivalent plastic strain versus pressure for corrosion diameter of 6 inches and cladding thickness of 0.240 inch

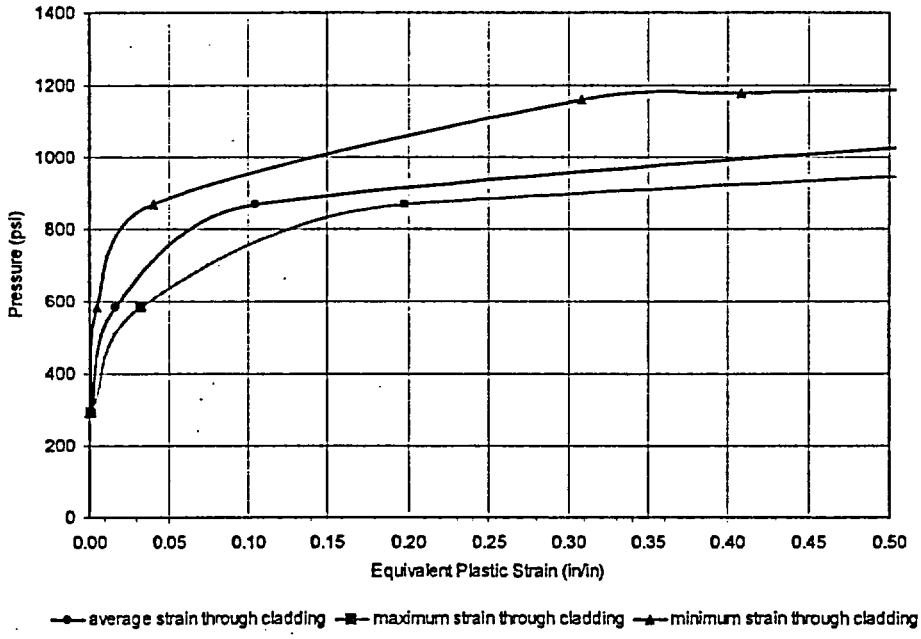

Figure B 14 Equivalent plastic strain versus pressure for corrosion diameter of 6 inches and cladding thickness of 0.188 inch